

Isolation and manipulation of living adherent cells by micromolded magnetic rafts

Philip C. Gach, Yuli Wang, Colleen Phillips, Christopher E. Sims, and Nancy L. Allbritton

Citation: *Biomicrofluidics* **5**, 032002 (2011); doi: 10.1063/1.3608133

View online: <http://dx.doi.org/10.1063/1.3608133>

View Table of Contents: <http://scitation.aip.org/content/aip/journal/bmf/5/3?ver=pdfcov>

Published by the [AIP Publishing](#)

Articles you may be interested in

[Translocation of nanoparticles through a polymer brush-modified nanochannel](#)

Biomicrofluidics **6**, 034101 (2012); 10.1063/1.4732799

[A permalloy zigzag structure based magnetic bio-sensor](#)

J. Appl. Phys. **111**, 07E506 (2012); 10.1063/1.3676213

[Preface to Special Topic: Microsystems for manipulation and analysis of living cells](#)

Biomicrofluidics **5**, 031901 (2011); 10.1063/1.3641860

[Numerical investigation of flow-through immunoassay in a microchannel](#)

J. Appl. Phys. **107**, 034907 (2010); 10.1063/1.3284077

[Versatile optical manipulation system for inspection, laser processing, and isolation of individual living cells](#)

Rev. Sci. Instrum. **77**, 063116 (2006); 10.1063/1.2214961



AIP | APL Photonics

APL Photonics is pleased to announce
Benjamin Eggleton as its Editor-in-Chief



Isolation and manipulation of living adherent cells by micromolded magnetic rafts

Philip C. Gach,¹ Yuli Wang,¹ Colleen Phillips,¹ Christopher E. Sims,¹ and Nancy L. Allbritton^{1,2,a)}

¹*Department of Chemistry, University of North Carolina, Chapel Hill, North Carolina 27599, USA*

²*Department of Biomedical Engineering, University of North Carolina, Chapel Hill, North Carolina 27599, USA and North Carolina State University, Raleigh, North Carolina 27695, USA*

(Received 20 March 2011; accepted 19 April 2011; published online 20 September 2011)

A new strategy for magnetically manipulating and isolating adherent cells with extremely high post-collection purity and viability is reported. Micromolded magnetic elements (termed micrafts) were fabricated in an array format and used as culture surfaces and carriers for living, adherent cells. A poly(styrene-*co*-acrylic acid) polymer containing well dispersed magnetic nanoparticles was developed for creating the microstructures by molding. Nanoparticles of $\gamma\text{Fe}_2\text{O}_3$ at concentrations up to 1% wt./wt. could be used to fabricate micrafts that were optically transparent, highly magnetic, biocompatible, and minimally fluorescent. To prevent cellular uptake of nanoparticles from the magnetic polymer, a poly(styrene-*co*-acrylic acid) layer lacking $\gamma\text{Fe}_2\text{O}_3$ nanoparticles was placed over the initial magnetic micraft layer to prevent cellular uptake of the $\gamma\text{Fe}_2\text{O}_3$ during culture. The micraft surface geometry and physical properties were altered by varying the polymer concentration or layering different polymers during fabrication. Cells plated on the magnetic micrafts were visualized using standard imaging techniques including brightfield, epifluorescence, and confocal microscopy. Magnetic micrafts possessing cells of interest were dislodged from the array and efficiently collected with an external magnet. To demonstrate the feasibility of cell isolation using the magnetic micrafts, a mixed population of wild-type cells and cells stably transfected with a fluorescent protein was plated onto an array. Micrafts possessing single, fluorescent cells were released from the array and magnetically collected. A post-sorting single-cell cloning rate of 92% and a purity of 100% were attained. © 2011 American Institute of Physics.

[doi:[10.1063/1.3608133](https://doi.org/10.1063/1.3608133)]

I. INTRODUCTION

The ability to efficiently isolate cells or colonies from a mixed population for further expansion or analysis is a process common to many areas of biomedical research and biotechnology.¹ Examples of such endeavors include cloning of stem cells or genetically engineered cells for the development of cell lines and creation of animal models and isolation of tumor cells for genetic analysis.^{2,3} Admixing of cells with different characteristics from those of interest can lead to skewed or inaccurate results in such biological studies. In many cases, the cells of interest will be in low abundance among the population. For this reason, it is important to have a technique capable of identifying single cells with the desired characteristic, separating those cells from the unwanted cells and then collecting the cells with high purity for further expansion or analysis. Commonly used techniques for performing these types of cell isolation

^{a)}Author to whom correspondence should be addressed. Electronic mail: nlallbri@unc.edu. Tel: +1 919 966 2291; Fax: +1 919 962 2388.

procedures include limiting dilution, colony picking, and fluorescence-activated cell sorting (FACS).^{4–7} A number of new technologies for single-cell isolation have been developed in recent years but have yet to be widely adopted including laser micro-dissection or laser ablation,^{8,9} optical tweezers,¹⁰ dielectrophoresis,¹¹ and microarray technologies.^{12,13}

The use of magnetism as an external physical force for isolating cells is particularly attractive due to its simplicity, effectiveness, and ease of manipulation.¹⁴ Magnetic cell separation (MACS®) developed by Miltenyi Biotec and the related techniques such as magnetic columns, flow channels, arrays, and tweezers rely on magnetic particles bound to the surface of the cells or taken up by the cells to provide magnetic domains encompassing the cell for selective manipulation by an external magnet.^{15–21} Magnetic microdevices or microstructures have been fabricated as microtools for precise positioning of cells²² or as mobile structures termed “microtransporters,” “microcarriers,” or “microplates” for manipulation of cells.^{23–25} These microstructures, either fabricated from magnetic materials or doped with magnetic nanoparticles, have not yet been shown to be useful for isolating individual cells from a mixed population. Recently, an array of magnetic microstructures was developed in combination with our previous microarray technology for cell sorting by embedding magnetic nanoparticles within the micropallet array elements.^{26,27} The transparent microstructures served as sites for attaching adherent cells. After screening the entire array, the cells of interest could be selectively detached from the array using a pulsed laser and collected against gravity with an external magnet to produce very pure populations of collected cells.²⁶

While the micropallet array is an efficient approach for cell sorting, the platform is expensive and complicated as it requires a photolithographically defined array created in a cleanroom environment and a laser integrated into a high quality microscope. An inexpensive and robust platform, termed a “microraft array,” was recently developed by our group for the efficient isolation of viable, single cells or colonies from a mixed population.¹³ A simple dip-coating process was used to fabricate an array composed of a large number of micron-scale elements (the micrarafts) on a polydimethylsiloxane (PDMS) template. Within the array, the micrarafts serve as releasable culture sites for individual cells or colonies. After identification of target cells or colonies, micrarafts possessing cells of interest can be released with a needle inserted through the PDMS template. Following release, the micraraft is allowed to drop from the inverted array onto a collection vessel, such as a Petri dish via gravity. This method has been successful in sorting cells with extremely high collection efficiency (100%) and post-sorting single-cell proliferation capability (95%); however, loosely adherent cells on the array can become detached during the release and collection procedure reducing the purity of isolated cells. Impurity of the isolated cells is undesirable for many applications, such as the creation of stably transfected cell lines. Re-sorting can be generally used to improve purity but results in cell loss and requires additional time and effort. To overcome this problem, magnetism was evaluated as a means to collect the released micrarafts and their adherent cells or colonies to achieve high purity of the collected cells. In the current article, the micraraft array platform was enhanced by doping the micraraft material with magnetic nanoparticles. The dispersion of nanoparticles inside the polymer matrix of the micrarafts and the resultant optical properties were examined. The fabrication of magnetic micraraft arrays *via* the dip-coating process was tested. An array of two-layer micrarafts composed of a magnetic base and a non-magnetic surface was fabricated to provide an optimal, nanoparticle-free culture surface. Imaging of cells by brightfield, fluorescence, and confocal microscopy was demonstrated. Finally, isolation and magnetic manipulation of single, viable cells from the array was demonstrated, and the purity of isolated cells was determined.

II. MATERIALS AND METHODS

A. Materials

The following materials were obtained from the Aldrich Chemical Company (St. Louis, MO): iron(II) chloride tetrahydrate (99%), iron(III) chloride anhydrous (98%), iron(III) nitrate nonahydrate (99+%), 28% ammonium hydroxide solution, oleic acid (90%), toluene (reagent grade), triarylsulfonium hexafluorophosphate salts (mixed, 50% in propylene carbonate), 99+% pure γ -butyrolactone (GBL), 1-methoxy-2-propanol (1002F developer, 98.5%), glutaraldehyde,

rhodamine B, 2,2'-azobisisobutyronitrile (AIBN, 98%), styrene ($\geq 99\%$), and acrylic acid (99.5%). EPON resin SU-8 and EPON resin 1002F (phenol, 4,4'-(1-methylethylidene)bis-, polymer with 2,2'-[(1-methylethylidene)bis(4,1-phenyleneoxymethylene)]bis-[oxirane]) were obtained from Miller-Stephenson (Sylmar, CA). Dulbecco's modified eagle medium (DMEM), fetal bovine serum (FBS), $1 \times$ phosphate buffered saline (PBS) pH 7.4, 0.05% trypsin with EDTA solution, penicillin/streptomycin, CellTrackerTM Red CMTPX, CellMaskTM Orange plasma membrane stain, and Hoechst dye No. 33342 were obtained from Invitrogen (Carlsbad, CA). Draq-5 DNA dye was from Biostatus (Leicestershire, UK). Poly(dimethylsiloxane) (PDMS, Sylgard 184 silicone elastomer kit) was purchased from Dow Corning (Midland, MI). Collagen I from rat tail tendon and FalconTM Petri dishes were purchased from BD Biosciences (San Jose, CA). Polycarbonate plates ($12'' \times 12'' \times 0.25''$) were purchased from McMaster-Carr (Los Angeles, CA). Wild-type HeLa cells were obtained from the American Type Culture Collection (ATCC, Manassas, VA). All other chemicals were procured from Fisher Scientific (Pittsburgh, PA).

B. Magnetic polystyrene development

Nanoparticles of Fe_3O_4 were synthesized by the co-precipitation of iron salts in deionized water through the addition of ammonium hydroxide.²⁸ The nanoparticles were magnetically decanted, and the fluid was replaced with fresh deionized water and iron nitrate. Mixing for 1 h at 80 °C in the presence of iron nitrate oxidized the nanoparticles to $\gamma\text{Fe}_2\text{O}_3$.²⁹ Magnetically decanting the nanoparticles and replacing the liquid with deionized water produced a magnetic ferrofluid. The nanoparticles were extracted with oleic acid to produce hydrophobic $\gamma\text{Fe}_2\text{O}_3$ nanoparticles. The magnetic phase was magnetically decanted, and excess oleic acid was removed by three washes in ethanol. The oleic acid-coated $\gamma\text{Fe}_2\text{O}_3$ nanoparticles were then dissolved in toluene (5 g of $\gamma\text{Fe}_2\text{O}_3$ /1L toluene). Poly(styrene-co-acrylic acid) (PS-AA) was prepared by copolymerization of styrene and acrylic acid in GBL, as described previously.¹³ Briefly 95 g styrene, 5 g acrylic acid, 0.1 g 2,2'-azobisisobutyronitrile (AIBN) and 100 g GBL were mixed in a flask and heated in a 60 °C water bath for 72 h to complete copolymerization. A 1:5 v/v mixture of PS-AA in toluene was slowly added to the $\gamma\text{Fe}_2\text{O}_3$ ferrofluid. The toluene was then evaporated (Büchi R200 rotovapor, Flawil, Switzerland) until a thick gel remained. GBL was added to this magnetic polystyrene gel until the desired viscosity for efficient dip coating was achieved.

C. Fabrication of magnetic microrrafts

Releasable magnetic microstructures were molded within PDMS microwells using a previously described protocol (see Supplemental materials).³⁰ For arrays composed of single-layer microrrafts, PS-AA, 1002F or SU-8 containing 1% $\gamma\text{Fe}_2\text{O}_3$ by weight was applied over the PDMS mold. Trapped air bubbles within the microwells were removed through degassing under vacuum (Oerlikon Leybold pump). The PDMS mold or template was then attached to a rotary DC motor and lowered into a solution of the magnetic polymer. Slowly raising the PDMS mold produced a convex solution of polymer isolated in each microwell as the template dewetted. Placing the PDMS mold in a 95 °C oven for 2 h evaporated the bulk of the GBL resulting in concave microstructures within the microwells. Further, evaporation of the GBL was achieved by a 1 h bake at 120 °C in a vacuum oven (-30 in. Hg). A magnetic microrraft developed with PS-AA containing 1% $\gamma\text{Fe}_2\text{O}_3$ dissolved in 75% GBL had a final $\gamma\text{Fe}_2\text{O}_3$ concentration of 4% by weight following evaporation of the GBL. For simplicity, the initial concentration of $\gamma\text{Fe}_2\text{O}_3$ in the PS-AA was used to define the magnetic loading throughout this report. Multi-layer microrrafts were constructed through repeated dip coating and drying of the array in various polymers dissolved in GBL.

Following fabrication of the microrraft arrays, the PDMS template was attached to a polycarbonate cassette, with the array facing toward the inside of the cassette. Slight stretching of the PDMS template during attachment to the cassette reduced sagging. While still attached to the cassette, a second polycarbonate structure to create a square inner chamber surrounding the

array (25.4 mm \times 25.4 mm \times 10 mm height—Fig. S4) was glued to the top of the mold using PDMS with a 70 °C bake for 1 h.³⁰

D. Release and collection of magnetic micrafts

Micrafts were released with the array in one of two orientations—inverted or upright. Micrafts on an inverted array were released by means of a microneedle (anodized steel, 150 μ m base diameter and 17.5 μ m tip diameter [Fine Science Tools, Foster City, CA]) positioned above the array and inserted through the PDMS template to dislodge the micraft which then settled on the collection dish, as previously reported.¹³ Release was followed by purification with an external magnet (see Supplemental materials for inverted-release purification).³⁰ Micrafts were also released from an upright array with the microneedle positioned below the array and above the objective of an inverted microscope (Fig. 6(a)). The microneedle was attached to a “U” brace on an XYZ micromanipulator. The visual field was kept clear of equipment except the microneedle by incorporating a 90° bend in the microneedle. Individual micrafts were released by raising the needle to puncture the PDMS template and dislodge the selected micraft. Following release, the microneedle was lowered to its original position so that the array could be translated with the microscope stage in preparation for the next release. An external magnet positioned above the collection substrate enabled immediate collection following micraft release (Fig. 5). The magnet was kept over the collection plate to retain micrafts in the collection chamber against gravity as the array and collection plates were separated.

E. Cell culture on magnetic micrafts

To expedite the attachment of cells to the micraft surface, the array was oxidized in a plasma cleaner (Harrick Plasma, Ithaca, NY) for 1 min. The micraft array and cassette holder were sterilized with 75% ethanol and allowed to dry in a tissue culture hood. Arrays were rinsed $\times 3$ with sterile deionized H₂O, and then 1 mL collagen in deionized H₂O (100 μ g mL⁻¹) was added to the array and incubated for 1 h including a 20 min degassing by vacuum to remove trapped air bubbles within the wells. Alternatively, plasma treatment and collagen coating can be omitted, but it took an extended period of time (>6 h) for cells to attach to the micraft surface. The arrays were rinsed $\times 3$ with deionized H₂O followed by the addition of DMEM supplemented with FBS (10%), L-glutamine (584 mg L⁻¹), penicillin (100 units mL⁻¹), and streptomycin (100 μ g mL⁻¹). A suspension of 15 000 cells was then added to the micraft array and allowed to settle and adhere to the micrafts over 2 h in a 37 °C incubator with a 5% CO₂ atmosphere. Cells used in these studies included wild-type HeLa cells, a human ovarian carcinoma cell line, HeLa cells stably transfected with enhanced green fluorescent protein (eGFP) fused to the nuclear H1-histone protein (a kind gift of Eva Lee, UC Irvine), and C2C12 cells, a murine myoblast cell line.

Prior to cell selection, the arrays were washed $\times 2$ with DMEM and then the chamber surrounding the array was filled with DMEM. A sterile polystyrene Petri dish was then mated to the micraft cassette to create a sealed chamber filled with cell culture media. Following the release procedure, the Petri dish containing the isolated micrafts/cells was removed from the cassette, immediately filled with 3 mL media, and was returned to a tissue culture incubator for continued culture of the cells.

F. Imaging of cells on magnetic micrafts

HeLa cells grown on micrafts and the expanded colonies were imaged by both brightfield and fluorescence microscopy using a cooled charge-coupled device (CCD) camera (Photometrics CoolSNAP HQ², Tucson, AZ) mounted to an inverted epifluorescence microscope (NIKON TE200-U, Melville, NY). Additionally, fluorescence microscopy was used to visualize HeLa cells co-labeled with Hoechst 33342 DNA dye and the cytoplasmic stain CellTrackerTM Red CMTPX. Fluorescently labeled C2C12 cells were imaged by differential interference contrast (DIC) and confocal microscopy with an inverted laser scanning microscope (Zeiss 510,

Thornwood, NY). After transient transfection with eGFP (see Supplemental materials), C2C12 cells were plated on microraft arrays and stained with CellMaskTM orange plasma membrane stain and Draq5 DNA dye following manufacturer protocols.³⁰ Fluorescence images were provided in pseudocolors representative of the fluorophore's excitation maximum wavelength.

III. RESULTS

A. Characterization of transparent magnetic polystyrene

A nanocomposite of uniformly distributed magnetic nanoparticles in a polystyrene:acrylic acid (PS-AA) co-polymer was developed to provide a magnetic and biocompatible material that could be molded into microstructures for cell culture and cell isolation. A ferrofluid containing superparamagnetic $\gamma\text{Fe}_2\text{O}_3$ nanoparticles and PS-AA in GBL was prepared as described above. Evaporation of the toluene left a composite of $\gamma\text{Fe}_2\text{O}_3$ nanoparticles up to 1 wt. % uniformly dispersed throughout a PS-AA matrix. This nanocomposite was then dissolved in GBL to provide a stable viscous media. The uniformity of the nanoparticle distribution in microrafts was confirmed by imaging films of the polymer under brightfield and with TEM. Films (100 μm thick) of the nanocomposite were transparent and slightly yellow when viewed using brightfield microscopy. TEM demonstrated well separated $\gamma\text{Fe}_2\text{O}_3$ nanoparticles (9 ± 4 nm, $n=97$) throughout the polymer with no aggregates above 30 nm (Figs. 1(a) and 1(b)).

Brightfield and fluorescence imaging are commonly employed for the detection of cells or other biological specimens. The compatibility of the polystyrene nanocomposite for these uses was assessed by measuring the background absorbance and fluorescence of 50- μm thick films with various concentrations of $\gamma\text{Fe}_2\text{O}_3$ spin-coated onto glass slides. Increases in the concentration of $\gamma\text{Fe}_2\text{O}_3$ from 0.01 to 1% showed corresponding increases in absorbance at shorter wavelengths. A nanocomposite containing 1% $\gamma\text{Fe}_2\text{O}_3$ reached 80% transmittance at a wavelength of 521 nm, whereas 0.1% $\gamma\text{Fe}_2\text{O}_3$ reached 80% transmittance at 425 nm (Fig. 1(c)). The fluorescence of the magnetic films was comparable to that of native PS-AA (data not shown).

Substrates for cell culture should provide good cellular adhesion and support long-term cell growth. Since AA possesses carboxylic acid groups, the surface of PS-AA will present a negative surface charge which should promote cell attachment without the need for surface oxidation or an extracellular matrix coating.^{13,31} Fourier transform infrared spectroscopy (FTIR) in the attenuated total reflectance (ATR) mode was used to assess the presence of carboxylic acid groups in the PS-AA copolymer. The absorption peak at 1704 cm^{-1} , characteristic of the carboxylic acid C=O stretch, was observed in films of both PS-AA and magnetic PS-AA, but not

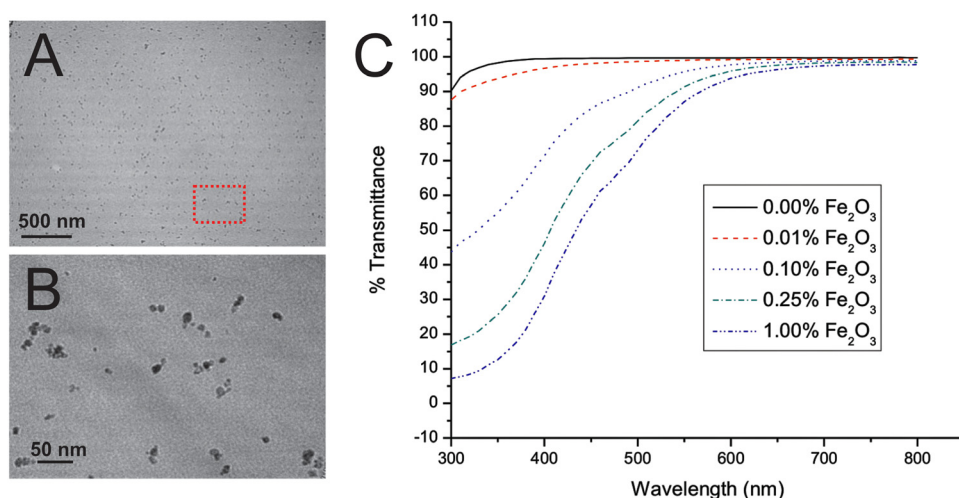


FIG. 1. Magnetic PS-AA characterization. (A) TEM image of PS-AA containing 1% $\gamma\text{Fe}_2\text{O}_3$ nanoparticles. (B) The region in the box in (A) is shown at increased magnification. (C) Transmittance curves of films of PS-AA with various concentrations of embedded $\gamma\text{Fe}_2\text{O}_3$ nanoparticles.

native polystyrene, demonstrating the retention of the polymer's negative charge with and without magnetic nanoparticle incorporation (Fig. S1).³⁰ HeLa cells plated on 1% $\gamma\text{Fe}_2\text{O}_3$ PS-AA showed adhesion 6 h after cell addition and well-formed colonies were present after 8 days in culture. These results demonstrated that PS-AA with 1% $\gamma\text{Fe}_2\text{O}_3$ was an excellent substrate for cell growth.

B. Single-layer magnetic rafts

Soft lithography has been used to develop a variety of microdevices for biomedical applications. Previously, micrafts on a PDMS substrate were developed to array and then isolate cells. In that work, a dip-coating process was used to fabricate microstructures from biocompatible polymers (SU-8, Epon 1002F epoxy resin, Epon 1009F epoxy resin, polystyrene or PS-AA) within an array of PDMS wells. The wells acted as a template to create the molded structures.¹³ In the current work, magnetic micrafts were created by dip-coating various polymers (SU-8, 1002F, and PS-AA) containing 0.01-1 wt. % uniformly distributed $\gamma\text{Fe}_2\text{O}_3$ nanoparticles dissolved in 70 wt. % GBL on a PDMS template consisting of an array of $100\ \mu\text{m} \times 100\ \mu\text{m}$ microwells isolated by walls $40\ \mu\text{m}$ tall and $20\ \mu\text{m}$ thick. The doped polymers showed successful dewetting on the PDMS as was required to construct the individual micrafts (Figs. 2(a) and S2).³⁰ Micrafts composed of PS-AA containing 1% $\gamma\text{Fe}_2\text{O}_3$ were isolated within the PDMS wells and possessed a slightly concave upper surface as monitored by SEM (Fig. 2(b)).

The transparency of the magnetic polymers was retained during micraft fabrication (Fig. 2(a)). It has previously been shown that magnetic nanoparticles can accumulate at the air interface of a polymer during photolithographic processing of magnetic photoresists.²⁶ Horizontal slices through the magnetic micrafts were imaged by TEM to determine whether a similar process might occur during raft fabrication. All micrafts composed of 1% $\gamma\text{Fe}_2\text{O}_3$ in 1002F showed evenly distributed nanoparticles throughout the polymer with the exception of a 20 nm layer of nanoparticles accumulated at the surface and base of the micrafts (Fig. S2).³⁰ These results confirmed the previous finding that nanoparticles are enriched at the surfaces of the

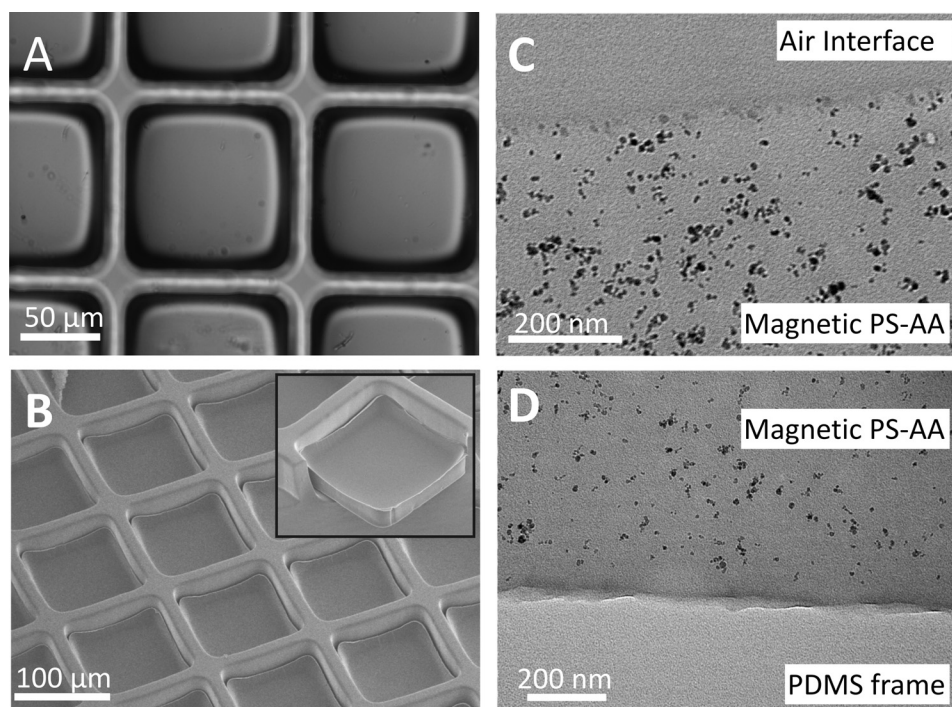


FIG. 2. Fabrication of magnetic micrafts. (A) Brightfield and (B) SEM images of PS-AA micrafts containing 1% $\gamma\text{Fe}_2\text{O}_3$. Inset shows a side view of a raft with PDMS partially removed. (C) TEM images of micraft-air interface and (D) PDMS-micraft interface.

1002F nanocomposite.²⁶ In contrast, micrafts developed with 1% $\gamma\text{Fe}_2\text{O}_3$ in PS-AA possessed uniformly distributed nanoparticles throughout the polymer without noticeable accumulation of nanoparticles at the micraft surface or base (Figs. 2(c) and 2(d)). It is likely that $\gamma\text{Fe}_2\text{O}_3$ nanoparticles were trapped within the viscous PS-AA matrix during GBL evaporation, whereas the particles in the 1002F monomer were mobile until the resist was exposed to UV light. Since the magnetic PS-AA more closely mimics the oxidized polystyrene surfaces for conventional tissue culture relative to the 1002F surface, the fabrication of micrafts with magnetic PS-AA was the focus of the remainder of this work.

C. Two-layer magnetic rafts

The application of layers of materials onto the surface of microdevices permits tailoring of surface properties for specific device functions. For example, a layer of native 1002F polymer applied over a magnetic 1002F surface was previously shown to provide a protecting layer to prevent nanoparticle uptake by cells.²⁶ Two-layer micrafts were constructed using sequential dip coating of the PDMS mold. Micrafts were initially formed by dip coating the mold into PS-AA containing 1% $\gamma\text{Fe}_2\text{O}_3$. A layer of PS-AA was then overlaid onto the magnetic micrafts using a second dip coating step (Fig. 3(a)). Following evaporation of solvent, a uniform layer of PS-AA was coated on the magnetic micraft (Fig. 3(b)). The polymer remained isolated within the PDMS wells and the micrafts retained smooth side walls as confirmed by SEM (Fig. 3(c)). The central thickness of the 1% $\gamma\text{Fe}_2\text{O}_3$ -PS-AA and PS-AA layers were 10 and 8 μm , respectively as measured by TEM (Fig. 3(d)). While the viscosities of the solutions used for the first and second layers were identical, the PS-AA layer was thinner since the effective depth of the well was decreased during the second dip coating step. The thickness of the micraft layers could be adjusted by controlling the concentration of polymer dissolved in

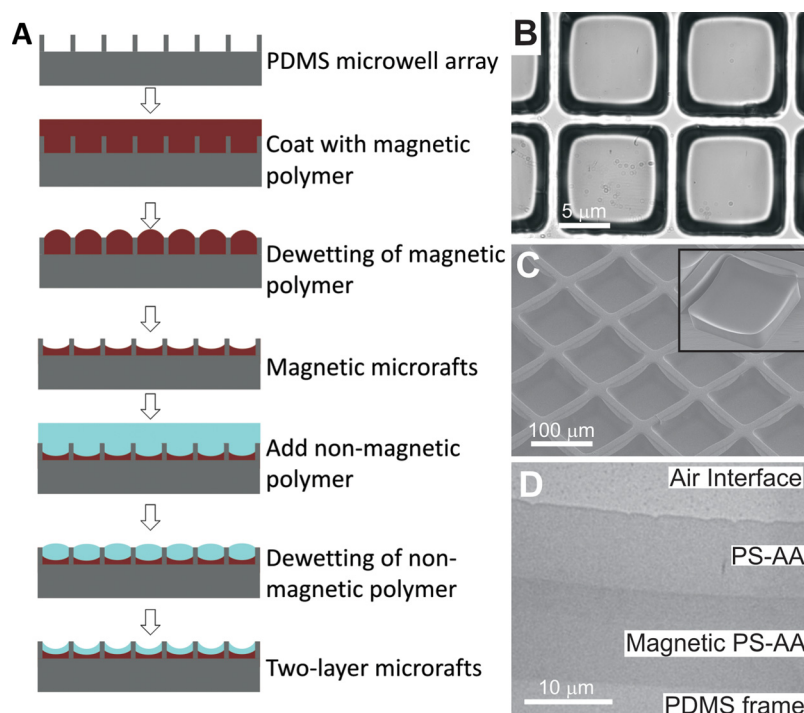


FIG. 3. Two-layer magnetic raft fabrication. (A) Scheme of two-layer micraft fabrication. (B) Brightfield and (C) SEM images of a 2-layer micraft composed of a 1% $\gamma\text{Fe}_2\text{O}_3$ in PS-AA as the base with a PS-AA top layer. Inset shows a side view of a 2-layer micraft with PDMS partially removed. (D) TEM image of a cross section of a 2-layer micraft composed of a 10 μm magnetic PS-AA layer covered with an 8 μm thick layer of PS-AA.

GBL during dip coating. For example, addition of PS-AA dissolved in 80 wt. % GBL resulted in a second layer thickness of 3 μm (data not shown).

D. Cell culture on magnetic rafts

Effective devices for culturing and isolating individual cells and cell colonies must be capable of providing both good cellular adhesion and supporting long-term growth on the substrate. PS-AA has previously been shown to be a biologically compatible substrate.¹³ This substrate can also be coated with extracellular matrices, such as fibronectin and collagen, to further improve cell adherence and growth. HeLa cells plated on magnetic PS-AA micrafts coated with collagen adhered to and spread across the surface of the micrafts within 2 h of plating as observed by brightfield microscopy and SEM (Figs. 4(a) and 4(b)). However, plasma treatment or the addition of an extracellular matrix (ECM) also modified the surface of the PDMS walls which reduced their barrier function in keeping the cells localized to individual micrafts. Thus, HeLa cells cultured on arrays treated by oxidation or ECM adsorption were observed to spread across the PDMS wall to adjacent micrafts after three days in culture. On the other hand, native PS-AA and magnetic PS-AA allow cellular adhesion within 6 h of plating without surface modification (Fig. 4(c)). Colonies of HeLa cells grown on these surfaces remained isolated on the micraft surface and within the confines of the PDMS walls for up to six days.

Many biological assays rely on fluorescent markers to identify the cells of interest. The ability to perform fluorescence imaging on two-layer magnetic rafts was demonstrated by examining cells loaded with fluorescence dyes using both epifluorescence and confocal microscopy. Cells plated on two-layer magnetic micrafts were stained with a nuclear dye (Hoechst 33342, excitation/emission 350/461 nm) and a cytoplasmic dye (CellTracker Red, excitation/emission 570/602 nm). Imaging by brightfield and fluorescence microscopy demonstrated the visualization of cellular detail on two-layer micrafts (Fig. S3).³⁰ The ability to perform fluorescence confocal imaging of cells on two-layer micrafts was demonstrated using C2C12 cells transfected with a fluorescent protein and co-labeled with nuclear and membrane dyes. C2C12 cells transiently transfected with eGFP (excitation/emission 492/517 nm) were plated on unmodified two-layer micrafts then stained with CellMaskTM orange plasma membrane dye (excitation/

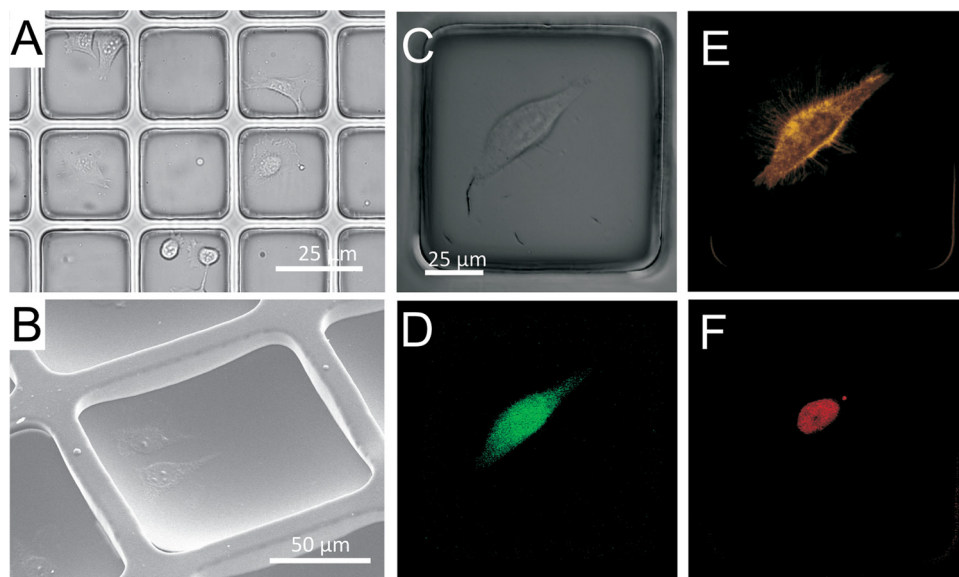


FIG. 4. Imaging cells on magnetic micrafts. Brightfield (A) and SEM (B) images of HeLa cells adhered to 2-layer micrafts (100 μm) coated with collagen. DIC (C) and confocal fluorescence (D)–(F) images of a C2C12 cell loaded with fluorescent dyes. Individual fluorescent channels show the fluorophores introduced to the cell by transfection with an eGFP expressing plasmid (emission at 517 nm) (D), staining with CellMaskTM orange plasma membrane dye (emission 567 nm) (E) and DNA staining (Draq-5 emission at 697 nm) (F).

emission 554/567 nm) and a DNA dye (Draq-5, excitation/emission 646/697 nm). Confocal images showed clear compartmentalization of the dyes without distortion despite imaging through the micrafts (Figs. 4(d)–4(f)).

E. Release and collection of magnetic micrafts

The utility of magnetic micrafts relies upon the ability to selectively release and manipulate them with an external magnet. Using a magnetic collection approach can also provide a method for purifying collected cells from non-target cells that may be shed from the array during the collection procedure. Single-layer magnetic micrafts were released in inverted and upright orientations. The efficiency of collection of released magnetic microstructures under varying magnetic field strengths and different concentrations of $\gamma\text{Fe}_2\text{O}_3$ was examined (Supplemental materials Table 1).³⁰ Using the upright approach as an example, the micrafts were

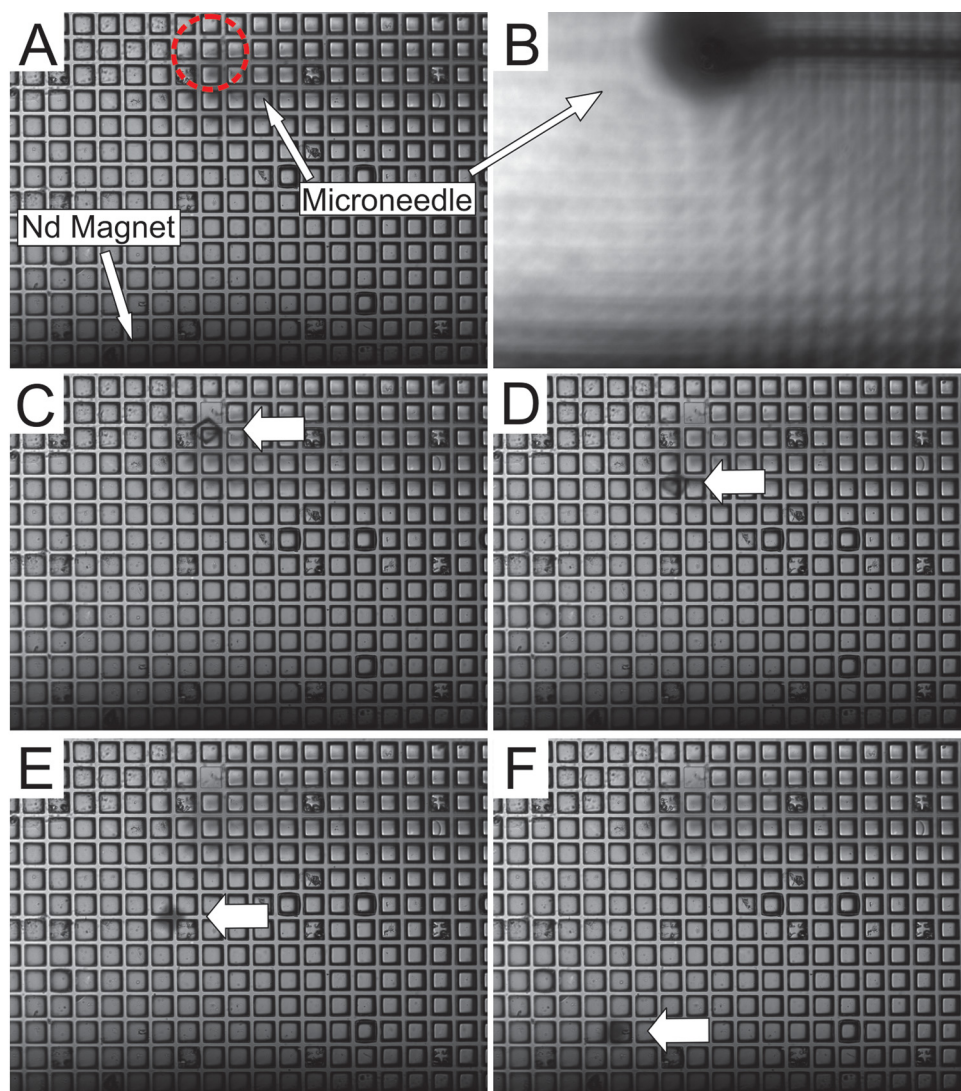


FIG. 5. A series of time-resolved images demonstrating the release and magnetic collection of micrafts. In the displayed images, the neodymium magnet shown at the bottom of the image is 5 mm above the array and out of the focal plane. The micraft array composed of PS-AA containing 0.1% $\gamma\text{Fe}_2\text{O}_3$ (A) is deflected out of the focal plane by the microneedle during release of an individual micraft (B). The position of the micraft 1, 2, 3, and 4.3 s following release, panels (C)–(F), respectively, was monitored to assess the movement of a loose magnetic microstructure in a magnetic field. Micrafts are observed to move upward and thus out of focus as they are attracted to the magnet (enhanced online). [URL: <http://dx.doi.org/10.1063/1.3608133.1>]

released and immediately collected onto a glass surface by an external magnet when the magnetic force experienced by the micrafts was sufficient to overcome gravitational force, as shown in Fig. 5. In triplicate experiments, 20 micrafts were released and then magnetically collected in this manner. Micrafts containing 1% $\gamma\text{Fe}_2\text{O}_3$ were collected with 100% efficiency ($n = 60$) at magnet displacements up to 20 mm, corresponding to a magnetic field of 22 mT at the glass surface. Increasing the distance between the glass surface and the collection plate to 24 mm (18 mT) reduced the collection efficiency to $28\% \pm 17\%$. Decreasing the concentration of $\gamma\text{Fe}_2\text{O}_3$ to 0.1% required reducing the distance between the collection plate and glass slide to 6 mm (166 mT) in order to achieve a collection efficiency of $100\% \pm 0\%$. Micrafts containing 0.01% $\gamma\text{Fe}_2\text{O}_3$ were not successfully collected when magnet separations down to 1 mm (449 mT) were attempted. Two-layer micrafts composed of 1% magnetic PS-AA bottoms and PS-AA tops produced collection probabilities of 100% at distances up to 16 mm (35 mT) and $73\% \pm 12\%$ at 20 mm (22 mT).

F. Cell sorting and purification with magnetic micrafts

Direct collection of cells on micrafts whether or not a magnet is employed has been shown to be efficient, but purity may be limited due to non-target cells being shed from the array during the release procedure. To assess the viability and purity of single cells isolated from the array by magnetically enhanced collection, cell isolation experiments were performed using a heterogeneous population of cells plated on the array (Fig. 6(a)). A minority population of HeLa cells stably expressing a nuclear eGFP was admixed with wild-type HeLa cells at a 1:3 ratio. To maximize the number of micrafts containing only a single cell, 15 000 cells were plated on an array of 44 000 two-layer micrafts (PS-AA top/1% magnetic PS-AA bottom) coated with collagen (Figs. 6(b)–6(e)). In three independent experiments, 60 micrafts

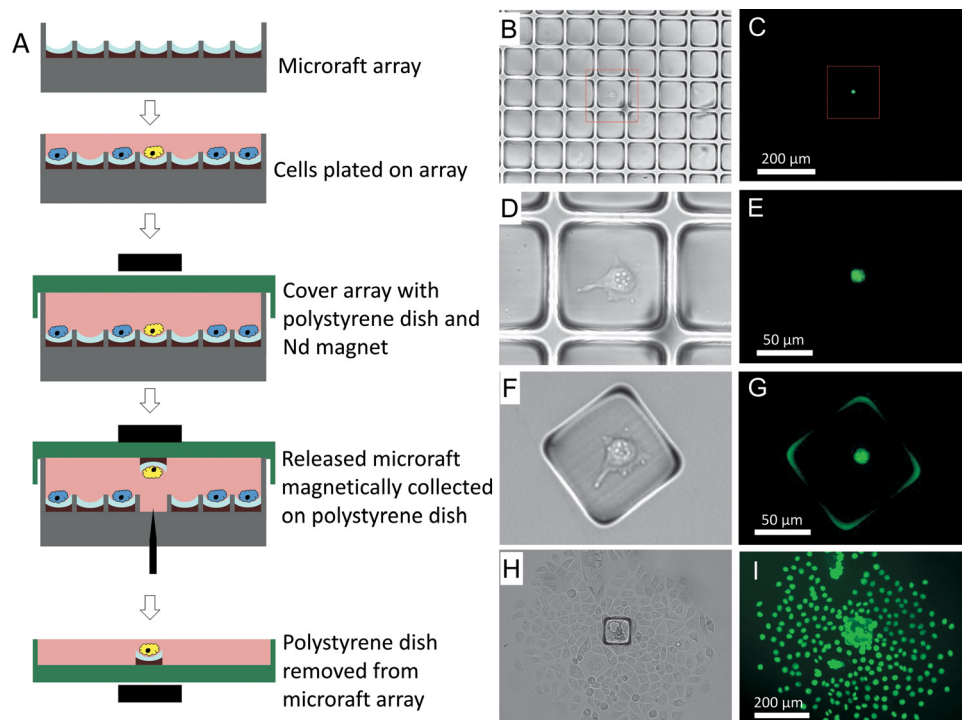


FIG. 6. Single cell sorting with magnetic micrafts. (A) Scheme for the magnetic collection of micrafts. (B)–(H) Bright-field and fluorescence images of a HeLa cell expressing a fluorescent protein identified, isolated and expanded in a clonal colony. (B)–(E) A single HeLa cell possessing a fluorescent nucleus is identified on an array composed of two-layer micrafts (100 μm). (F)–(I) The cell seen in “(B)–(E)” immediately following magnetic-assisted collection (F), (G) and after 7 days of incubation (H), (I).

containing a single cell possessing a fluorescent nucleus were released. Immediately after the collection procedure, all released micraft retained their attached cell (Figs. 6(f) and 6(g)). After 7 days, 55 of the single cells ($92\% \pm 5\%$) had expanded into a colony in which all cells possessed fluorescent nuclei with no non-fluorescent cells admixed (Figs. 6(h) and 6(i)). Selective isolation of cells attached to magnetically collected micrafts was confirmed by releasing and magnetically collecting 20 micrafts without adherent cells from the micraft array plated with cells. Following 7 days culture, no cell colonies were observed on the collection plate. A cell collection efficiency of 100% with 100% purity and a single-cell cloning efficiency of 92% was attained demonstrating the feasibility of creating highly purified clonal populations of cells from a heterogeneous population.

IV. CONCLUSIONS

Magnetic microstructures were developed to enhance the manipulation and purity of cells isolated from a cell-based microarray. Nanoparticles composed of $\gamma\text{Fe}_2\text{O}_3$ were uniformly dispersed in a polystyrene-based polymer to provide biocompatible, transparent, magnetic micrafts. Through the use of multiple dip-coatings, micrafts composed of multiple layers could be easily fabricated. In this manner, micrafts were created with layers composed of differing properties. For example, application of a polymer layer lacking nanoparticles over the magnetic layer overcame potential cell uptake of $\gamma\text{Fe}_2\text{O}_3$ from the culture surface. Viable cells cultured on the arrays of single- or two-layer magnetic micrafts could be viewed by brightfield, fluorescence and confocal imaging for identification and selection. Upon release, selected cells were magnetically collected efficiently and with high viability to achieve single-cell cloning rates of 92%. The magnetic properties of the micrafts enabled the attached cells to be readily separated from any contaminating cells shed from the array during the identification and release procedures. The magnetically enhanced retrieval process enabled 100% purity of collected cells to be achieved. These results demonstrated the utility of using magnet micrafts for obtaining highly pure and viable cells for cloning applications.

ACKNOWLEDGMENTS

This research was supported by grants from the National Institutes of Health (EB007612 and EB012549). We thank Dr. Joe Kornegay for supplying the CMV driven eGFP expression plasmid and David Detwiler for his assistance with C2C12 cell transfection. Dr. Michael Chua, director of the Hooker Microscopy Facility, is acknowledged for his assistance with DIC and confocal imaging. Dr. Mark Walters, director of the Shared Materials Instrumentation Facilities at Duke University, is recognized for his acquisition of ATR-FTIR spectra. N.L.A, C.E.S, and Y.W. disclose a financial interest in Cell Microsystems, Inc.

- ¹D. Patel, *Separating Cells* (Springer-Verlag, New York, 2001).
- ²K. Mori, A. Kashiwagi, and T. Yomo, *J. Eukaryot. Microbiol.* **58**(1), 37 (2010).
- ³S. Nagrath, L. V. Sequist, S. Maheswaran, D. W. Bell, D. Irimia, L. Ulkus, M. R. Smith, E. L. Kwak, S. Digumarthy, A. Muzikansky, P. Ryan, U. J. Balis, R. G. Tompkins, D. A. Haber, and M. Toner, *Nature* **450**(7173), 1235 (2007).
- ⁴R. I. Freshney, *Culture of Animal Cells* (Wiley-Liss, New York, 2000).
- ⁵H. M. Shapiro, *Practical Flow Cytometry*, 4th ed. (Wiley-Liss, New York, 2003).
- ⁶A. L. Givan, *Flow Cytometry First Principles*, 2nd ed. (Wiley-Liss, New York, 2001).
- ⁷D. J. Kirkland, *Br. J. Cancer* **34**, 134 (1976).
- ⁸K. Schutze, H. Posl, and G. Lahr, *Cell. Mol. Biol.* **44**(5), 735 (1998).
- ⁹J. S. Kim, D. Hur, J. K. Hwang, C. Chung, and J. K. Chang, *Bioanalysis* **2**(10), 1755 (2010).
- ¹⁰J. R. Kovac and J. Voldman, *Anal. Chem.* **79**, 9321 (2007).
- ¹¹P. R. C. Gascoyne, X. B. Wang, Y. Huang, and F. F. Becker, *IEEE Trans. Ind. Appl.* **33**(3), 670 (1997).
- ¹²Y. L. Wang, G. Young, P. C. Aoto, J. H. Pai, M. Bachman, G. P. Li, C. E. Sims, and N. L. Allbritton, *Cytometry A* **71A**(10), 866 (2007).
- ¹³Y. L. Wang, C. Phillips, W. Xu, J. H. Pai, R. Dhopeswarkar, C. E. Sims, and N. Allbritton, *Lab Chip* **10**(21), 2917 (2010).
- ¹⁴J. T. Kemshead and J. Ugelstad, *Mol. Cell. Biochem.* **67**, 11 (1985).
- ¹⁵S. Miltenyi, W. Muller, W. Weichel, and A. Radbruch, *Cytometry* **11**(2), 231 (1990).
- ¹⁶W. Liu, N. Dechev, I. G. Foulds, R. Burke, A. Parameswaran, and E. J. Park, *Lab Chip* **9**(16), 2381 (2009).
- ¹⁷J. D. Adams, P. Thevoz, H. Bruus, and H. T. Soh, *Appl. Phys. Lett.* **95**, 254103 (2009).
- ¹⁸D. C. Pregibon, M. Toner, and P. S. Doyle, *Langmuir* **22**(11), 5122–8 (2006).

- ¹⁹K. Ino, M. Okochi, N. Konishi, M. Nakatochi, R. Imai, M. Shikida, A. Ito, and H. Honda, *Lab Chip* **8**(1), 134 (2008).
- ²⁰H. Lee, Y. Liu, D. Ham, and R. M. Westervelt, *Lab Chip* **7**(3), 331 (2007).
- ²¹N. Xia, T. P. Hunt, B. T. Mayers, E. Alsberg, G. M. Whitesides, R. M. Westervelt, and D. E. Ingber, *Biomed. Microdevices* **8**(4), 299 (2006).
- ²²M. Hagiwara, T. Kawahara, Y. Yamanishi, and F. Arai, *Appl. Phys. Lett.* **97**, 0137013 (2010).
- ²³M. S. Sakar, E. B. Steager, D. H. Kim, M. J. Kim, G. J. Pappas, and V. Kumar, *Appl. Phys. Lett.* **96**, 043705 (2010).
- ²⁴L. N. Kim, S. E. Choi, J. Kim, H. Kim, and S. Kwon, *Lab Chip* **11**(1), 48 (2011).
- ²⁵H. Ishihara and S. Takeuchi, in IEEE MEMS 2010 Conference, Hong Kong, China, 24-28 January 2010, p. 959.
- ²⁶P. C. Gach, C. E. Sims, and N. L. Allbritton, *Biomaterials* **31**(33), 8810 (2010).
- ²⁷N. M. Gunn, R. Chang, T. Westerhof, G. P. Li, M. Bachman, and E. I. Nelson, *Langmuir* **26**(22), 17703 (2010).
- ²⁸R. Massart, *IEEE Trans Magn.* **17**, 1247 (1981).
- ²⁹A. Bee, R. Massart, and S. Neveu, *J. Magn. Magn. Mater.* **149**, 6 (1995).
- ³⁰See supplementary material at <http://dx.doi.org/10.1063/1.3608133> for PDMS template fabrication, measurement of magnetic polystyrene absorption, ART-FTIR procedure, SEM and TEM sample preparation, cell transfection, ATR-FTIR of magnetic PS-AA, microraft fabrication, fluorescence cell imaging, microraft array image, magnetic purification of collected microrafes, and magnetic purification of cells on microrafes.
- ³¹H. Jung, B. Kwak, H. S. Yang, G. Tae, J. S. Kim, and K. Shin, *Colloid Surf. A* **313**, 562 (2008).